Neutron total cross section of ^{40}Ca and cross section difference of ^{44}Ca$-^{40}$Ca

H. S. Camarda
The Pennsylvania State University, Delaware County Campus, Media, Pennsylvania 19063
and University of California, Lawrence Livermore National Laboratory, Livermore, California 94550

T. W. Phillips and R. M. White
University of California, Lawrence Livermore National Laboratory, Livermore, California 94550
(Received 16 September 1985)

We have used a 100-MeV electron linac and neutron time-of-flight facility to measure the neutron total cross section of ^{40}Ca and the cross section difference of ^{44}Ca$-^{40}$Ca for incident neutron energies of 6–60 MeV. Optical model calculations of ^{40}Ca σ_T have been made and compared to the data. Modifications of a global set of optical model parameters necessary to fit the ^{44}Ca$-^{40}$Ca difference data are discussed. Using these parameters we calculated $\Delta=\langle r^2\rangle_{44}^{1/2}-\langle r^2\rangle_{40}^{1/2}$ for the real part of the potential and found a value of 0.16 ± 0.05 fm. The value of Δ is sensitive to the difference in the matter distribution of the ^{44}Ca and ^{40}Ca nuclei and our result is consistent with the same quantity determined from low energy alpha particle scattering.

I. INTRODUCTION

Calcium isotopes have been studied in scattering experiments using a variety of probes.[1] The optical potentials derived from these studies can be viewed as convolutions of the effective interaction between the probe and target nucleons and the nucleon density of the target nucleus.[2] For electromagnetic probes, the interaction is the Coulomb force and the density being probed is the charge. For hadronic probes the effective interaction is more complicated. Simple arguments predict that neutrons will be most sensitive to the proton density and protons to the neutron density. A conference[1] reviewing the state of knowledge of nucleon distributions in calcium isotopes contained no reference to neutron experiments.

We have carried out an absolute neutron total cross section (σ_T) measurement on ^{40}Ca along with a neutron total cross section difference ($\Delta\sigma_T$) measurement for ^{44}Ca$-^{40}$Ca over the energy range 6–60 MeV. The method and purpose of this work is similar to that which is described in a previous publication.[3] Namely, we use an optical model analysis of the absolute σ_T data to fix the parameters of an optical potential and then change the parameters of the potential in order to fit the cross section difference data. Through this analysis we try to learn about differences between nuclei which differ by a few nucleons. In Ref. 3 we reported a σ_T measurement of ^{140}Ce, and $\Delta\sigma_T$ measurements for ^{139}La$-^{140}$Ce, ^{141}Pr$-^{140}$Ce, and ^{142}Ce$-^{140}$Ce from 3 to 60 MeV. We found that the ^{139}La$-^{140}$Ce and ^{141}Pr$-^{140}$Ce data could be fitted well by making the small changes in the geometrical parameters and isospin term of the potential implied by the removal or addition of a single proton to ^{140}Ce. The fit to the ^{142}Ce$-^{140}$Ce data required a more abrupt change of the optical potential parameters. This is reasonable considering the fact that ^{142}Ce differs from ^{140}Ce by the addition of two neutrons beyond the closed $N=82$ neutron shell. In the analysis presented here we examine the changes to an optical potential, which fits the σ_T^{40} data, required to fit the ^{44}Ca$-^{40}$Ca $\Delta\sigma_T$ data where four neutrons have been added to the doubly-closed-shell ^{40}Ca nucleus. We compare this study using the neutron as a probe to other studies of the calcium isotopes which used different probes.

II. EXPERIMENTAL DETAILS

A 110-MeV electron beam from the Lawrence Livermore National Laboratory linear accelerator struck a Ta-Be target producing a white source of neutrons whose energies were determined using the time-of-flight technique. The neutron-producing target was viewed along 15 and 250 m flight paths. The 15 m flight path was used to monitor the neutron flux, and the neutron detector for the total cross section measurements was located at 250 m. The 250 m detector consisted of an array of 16 separate scintillators $25.4\times25.4\times5.1$ cm thick placed directly in the neutron beam. Each scintillator was viewed by two phototubes operating in a coincidence mode. The accelerator was operated at 1440 pulses per sec with a 12-nsec beam-pulse width and an average current of 55 μA on the Ta-Be neutron producing target. The number of neutrons detected was stored by arrival time in spectra whose channel widths varied from 4 nsec at the highest energies to 64 nsec at low energies. A detailed description of the time-of-flight facility, neutron production target, detector, and data acquisition system used for these measurements is given in Ref. 3.

III. CROSS SECTION MEASUREMENTS

A. Total cross section measurement

One of the reasons for making an accurate measurement of the ^{40}Ca neutron total cross section was to obtain quality data over the energy range of interest to which an

TABLE I. Number of atoms/barn, n, for each element in our samples.

Sample	Element	n (atoms/barn)
$^{40}CaCO_3$	^{40}Ca	0.1397
$^{40}CaCO_3$	^{42}Ca	0.0001
$^{40}CaCO_3$	^{44}Ca	0.0001
$^{40}CaCO_3$	C	0.1399
$^{40}CaCO_3$	O	0.4196
$^{44}CaCO_3$	^{40}Ca	0.0019
$^{44}CaCO_3$	^{44}Ca	0.1380
$^{44}CaCO_3$	C	0.1399
$^{44}CaCO_3$	O	0.4198

optical model fit could be made. Several measurements[4,5] of σ_T for natural Ca (96.94% ^{40}Ca) exist below 30 MeV, but above 30 MeV few published measurements are available.[6]

The ^{40}Ca sample, which contained 99.87% ^{40}Ca, was in the chemical form $CaCO_3$ and was placed in a cylindrical container with an inner diameter of 15 mm. Table I lists the thicknesses in units of atoms per barn for all our samples. The sample-in/sample-out technique was used to measure the cross section. The sample-out consisted of two separate samples, H_2O and C, with the number of oxygen and carbon atoms matched to that of the ^{40}Ca sample. The neutron beam was collimated down to 10 mm and the samples were placed 7 m from the Ta-Be target. As described in Ref. 3, the effect of hydrogen on the measured transmission was unfolded analytically. The uncertainty in our ^{40}Ca measurement receives its major contribution at low energies from the assumed 1% uncertainty of the n,p cross section. At the highest energy, the background subtraction contributed a 2% uncertainty. The net systematic uncertainty, $\delta(\sigma_T^{40})$, due to normalization errors, background subtractions, and $\sigma_{n,p}$ corrections, is 3% at low energies and 2.5% at high energies. These uncertainties are somewhat larger than those reported in Ref. 3 for the ^{140}Ce σ_T measurement. There are two principal reasons for this increase. First, the calcium samples were in the chemical form $CaCO_3$ (compared to CeO_2) and, consequently, required a larger $\sigma_{n,p}$ correction for the open (H_2O) sample. Further, the calcium cross section is a factor of 2 smaller than the Ce cross section and is therefore more sensitive to experimental uncertainties. Table II lists the ^{40}Ca total neutron cross section and statistical uncertainty as a function of neutron energy. To within the quoted errors our measurement is in agreement with other data at low[4,5] and high[6] energies.

TABLE II. ^{40}Ca experimental neutron total cross section and statistical uncertainty as a function of neutron energy.

E (MeV)	σ_T (b)	$\delta\sigma_T$ (b)
5.940	3.199	0.027
6.712	3.005	0.019
7.456	2.917	0.017
8.331	2.761	0.019
9.371	2.658	0.020
10.62	2.468	0.014
12.14	2.287	0.015
14.01	2.120	0.016
16.37	2.045	0.020
19.40	2.017	0.019
23.29	2.072	0.018
28.41	2.136	0.021
33.17	2.182	0.017
37.38	2.210	0.019
42.49	2.190	0.023
48.76	2.136	0.024
56.57	2.075	0.046

B. Cross section difference measurements

The cross section difference (i.e., the transmission ratio of the samples) for nuclei which differ by a few nucleons can be measured very accurately. The important errors arise from run to run normalizations and sample thickness errors. Since the backgrounds of the two samples are similar, their effect on $\Delta\sigma_T$ cancel to a high degree.

After dead time corrections and background subtractions were made, the experimental transmission, T_R, was calculated. The cross section difference $\Delta\sigma_T=\sigma_T^{44}-\sigma_T^{40}$ can be expressed in terms of T_R and the constituents of the sample as

$$\Delta\sigma_T=\frac{1}{n_{44}^{44}-n_{44}^{40}}[\ln T_R-(n_{40}^{44}+n_{44}^{44})\sigma_T^{40}+(n_{40}^{40}+n_{42}^{40}+n_{44}^{40})\sigma_T^{40}-(n_c^{44}-n_c^{40})\sigma_T^{c}-(n_{ox}^{44}-n_{ox}^{40})\sigma_T^{ox}], \quad (1)$$

where the symbol n_{40}^{44} means the number of ^{40}Ca atoms/barn in the ^{44}Ca sample, etc. Table III lists the ^{44}Ca$-^{40}$Ca neutron total cross section difference data as a function of neutron energy calculated using Eq. (1).

TABLE III. ^{44}Ca$-^{40}$Ca experimental neutron total cross section difference and statistical uncertainty as a function of neutron energy.

E (MeV)	$\Delta\sigma_T=\sigma_T^{44}-\sigma_T^{40}$ (mb)	$\delta(\Delta\sigma_T)$ (mb)
5.09	183.8	19.5
6.18	198.9	10.1
7.18	127.4	8.5
8.39	173.5	9.1
9.74	127.0	6.5
11.56	157.8	6.4
13.98	179.7	7.2
17.23	169.4	6.5
21.80	146.7	6.9
28.07	171.3	8.4
34.22	185.4	12.4
40.31	193.3	17.4
48.29	246.3	24.0
58.99	247.3	52.8

In addition to the statistical uncertainty listed in Table III, $\Delta\sigma_T$ has a systematic uncertainty. The major contribution to the systematic uncertainty was due to normalization errors and was found to be 30 mb by comparing our $\Delta\sigma_T$ values for two separate runs. This is larger than the corresponding error for our $\Delta\sigma_T$ data of Ref. 3 and implies poorer beam stability during our calcium runs. This error combined with the sample thickness uncertainties ($\delta n/n = 7\times10^{-3}$) resulted in a net systematic uncertainty of 33 mb ($\sim$20%).

IV. OPTICAL MODEL CALCULATIONS

A. Total cross section calculations

In performing our optical model analysis, we first fitted the ^{40}Ca neutron total cross section over the energy range (6–60 MeV) of our experiment and then, the parameters of the potential were altered in order to fit the ^{44}Ca$-^{40}$Ca $\Delta\sigma_T$ data. Two potentials were used in order to examine the sensitivity of our results to the particular optical potential employed. We used the Ohio University (OU) global neutron potential of Rapaport *et al.*[7] (parameter set *A*), and an alternative potential also possessing both surface and volume absorption (SV) which is described in the Appendix. The calculations were performed with the code OPTICAL.[8]

In Ref. 3 the OU potential was used to fit the ^{140}Ce σ_T data between 3 and 60 MeV. Although the OU potential fit the ^{140}Ce total cross section well up to a neutron energy of 25 MeV, it was necessary to modify the potential in order to achieve a satisfactory fit above 25 MeV. Specifically, the strength of the volume absorption which increased linearly with neutron energy was changed to remain at the constant value of 5.2 MeV for neutron energies above 25 MeV. This slightly modified OU potential gave a good fit to the ^{40}Ca total cross section when the geometrical and strength parameters appropriate for ^{40}Ca were used. The results are shown in Fig. 1, where the solid line represents the OU potential and the dot-dashed line is the fit obtained with the SV potential as described in the Appendix. The fits to the data with each of these potentials are of good quality.

It is interesting to note that two equally good fits to σ_T data, using two different optical potentials, do not imply good agreement in the calculated reaction cross section, σ_R. We have plotted σ_R vs neutron energy for ^{40}Ca in Fig. 2. The solid and dot-dashed lines are calculations using the OU and SV potentials and the two data points are from Zanelli *et al.*[6] It is clear that the data lie between the different values of σ_R predicted by the OU and SV potentials.

B. Optical model fit to the difference cross section

Having obtained good fits to σ_T vs neutron energy for ^{40}Ca, we next investigated those changes required in the potential to reproduce the experimentally observed ^{44}Ca$-^{40}$Ca difference cross section. The solid line in Fig. 3 is $\Delta\sigma_T$ calculated using the OU potential by changing just N and A from ^{40}Ca to ^{44}Ca values. The calculated $\Delta\sigma_T$ does not fit the data and would still not fit even if each data point were lowered by our systematic uncertainty of 33 mb. The dashed line represents the calculated $\Delta\sigma_T$ where A was increased from 40 to 44 but where the $(N-Z)/A$ term in the real part of the potential was kept at the ^{40}Ca value, i.e., zero. The dotted curve was obtained by keeping the size of the nucleus fixed at the $A=40$ value, but letting the $(N-Z)/A$ term in the real part of the potential assume the ^{44}Ca value. The dashed and dotted curves of Fig. 3 illustrate the opposing effects which result in the solid line having a shape that more closely resembles the data. Similar results were found with the SV potential.

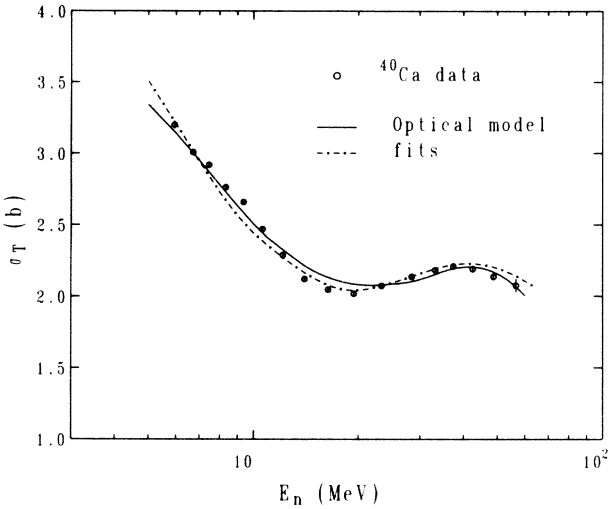

FIG. 1 The measured ^{40}Ca total neutron cross section as a function of energy. Statistical errors for these data are less than the size of the plotting symbol. The solid and dot-dashed lines represent optical model fits to the data using the OU and SV potentials as described in the text.

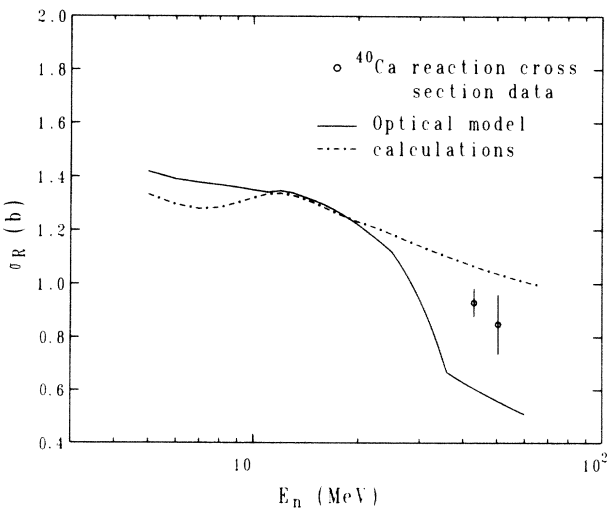

FIG. 2. Calculation of the ^{40}Ca reaction cross section as a function of neutron energy. The solid and dot-dashed line represent the calculated ^{40}Ca reaction cross section using the OU and SV optical potentials. The data points are from Ref. 6.

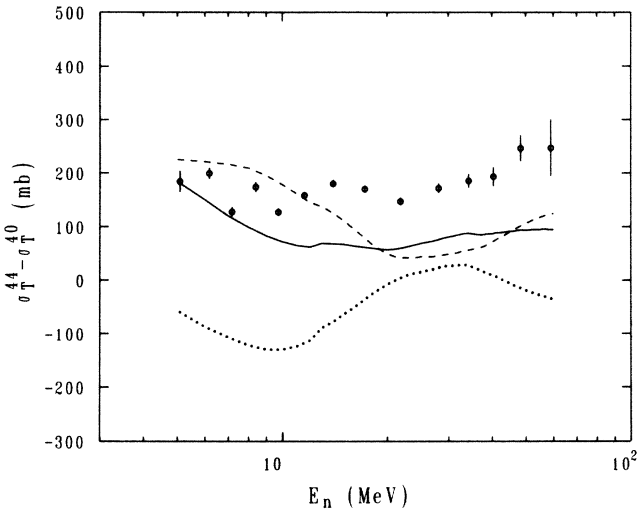

FIG. 3. The total neutron cross section difference of ^{44}Ca$-^{40}$Ca as a function of neutron energy. Using the OU potential the dashed line was calculated with A increased from 40 to 44 but with the $(N-Z)/A$ term in the real potential set equal to zero. Thus the dashed curve reflects the behavior of $\Delta\sigma_T$ due to the increased size of the ^{44}Ca nucleus. The dotted curve was obtained by keeping the size of the ^{44}Ca nucleus equal to that of ^{40}Ca, but letting the $(N-Z)/A$ term in the real potential assume the ^{44}Ca value. The solid line was calculated with both the increase in the size of the ^{44}Ca nucleus and the inclusion of the $(N-Z)/A$ term in the potential. It is clear that the line is the result of the two opposing effects.

Figure 4 shows our final fit to the difference data for both the OU and SV potentials. The changes required to fit the cross section difference were quite similar for both potentials. For the OU potential the diffuseness of the real, volume absorptive, and surface absorptive potentials were increased from 0.663 to 0.693 fm, 0.59 to 0.63 fm, and 0.59 to 0.63 fm, respectively. In addition, the standard OU potential strength for the $(N-Z)/A$ term in the real part of the potential which has the form $(22.7-0.19E)$ was changed to $(30-0.19E)$. This implies a stronger asymmetry term for ^{44}Ca than global fitting would imply. Although the highest energy data points of Fig. 4 have larger statistical uncertainties, the data clearly suggest an increasing $\Delta\sigma_T$ above 40 MeV. The increase in the calculated $\Delta\sigma_T$ at higher energies was achieved by decreasing, linearly with neutron energy, the strength of the ^{44}Ca volume absorption from the value of 5.2 MeV at $E=25$ MeV to 3.0 MeV at $E=50$ MeV. The necessity of having to increase the diffuseness of the real and imaginary parts of the potential to fit the ^{44}Ca$-^{40}$Ca data is the same as the changes required to fit the ^{142}Ce$-^{140}$Ce data of Ref. 3. Both ^{40}Ca and ^{140}Ce have closed neutron shells, and the additional neutrons will be found in new single-particle levels.

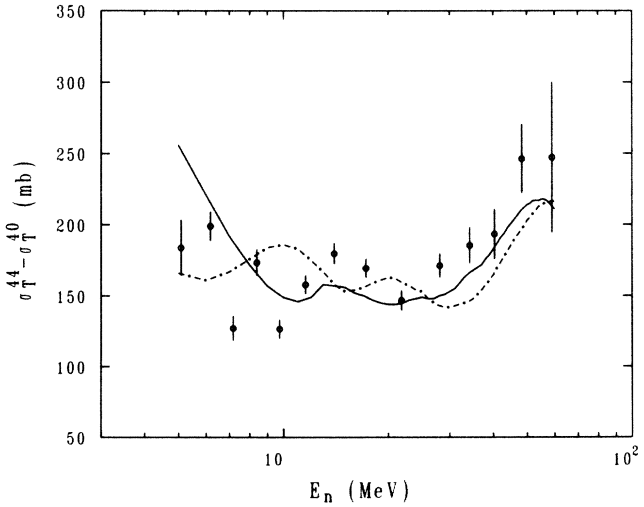

FIG. 4. The solid and dot-dashed lines represent the final fit to the ^{44}Ca$-^{40}$Ca difference data using the OU and SV potentials. For both calculations it was necessary to increase the diffuseness of the real and absorptive parts of the potentials.

V. DISCUSSION

If the proton number of the target nucleus being studied is changed, the neutron total cross section difference data are most sensitive to the change in the proton distribution. On the other hand, if the neutron number of the target nucleus is changed, the neutron difference data can be sensitive to the change in both the proton and the neutron distributions.

We have carried out a phenomenological analysis to compare our results with those of others. We have calculated the rms radius $\langle r^2\rangle^{1/2}$ for ^{40}Ca and ^{44}Ca, where $\langle r^2\rangle$ is

$$\langle r^2\rangle = \int r^2 V(r)d\mathbf{r} \Big/ \int V(r)d\mathbf{r}\,, \tag{2}$$

and $V(r)$ is the real part of the potential. Letting $\Delta=\langle r^2\rangle_{44}^{1/2}-\langle r^2\rangle_{40}^{1/2}$ we find that $\Delta=0.15$ fm and 0.17 fm for the OU and SV potentials. The 33 mb uncertainty of the difference data leads us to an uncertainty in Δ of ±0.05 fm. Thus our final value for the difference in rms radii for ^{44}Ca and ^{40}Ca is $\Delta=0.16\pm0.05$ fm. We note that Δ is sensitive to the difference between the neutron and proton distributions of ^{44}Ca and ^{40}Ca. An optical model analysis of low energy alpha particle scattering,[9] carried out in a manner similar to ours, yielded a value of the difference in rms radii for ^{44}Ca and ^{40}Ca of 0.11 ± 0.06 fm. This agreement is satisfactory considering the errors in both measurements and the uncertainties associated with an optical model analysis.

A similar result was obtained from proton scattering[10] where values of the difference in rms radii for ^{44}Ca and ^{40}Ca of 0.11 fm and 0.16 fm were obtained by two different optical model analyses of the same data. Electromagnetic probes[11] give a smaller difference (~0.04 fm) for these two isotopes and indicate that the charge distribution has changed slightly. The proton, alpha-particle, and neutron difference data, which are sensitive to changes in the neutron and proton distributions, suggest a larger change in the neutron distribution than the proton distribution. However, to extract the change in the distributions from ^{40}Ca to ^{44}Ca, a microscopic analysis which incorporates the details of the effective interaction will be essential.

VI. SUMMARY

We have measured the ^{40}Ca total cross section over the energy range 6–60 MeV with a systematic uncertainty of $\sim 3\%$. We have also measured the ^{44}Ca$-^{40}$Ca total cross section difference over the same energy range with a systematic uncertainty of $\sim 20\%$.

Optical model calculations of ^{40}Ca σ_T, using two different potentials, are in good agreement with the σ_T data. However, minor and reasonable changes of the optical potential parameters did not yield a satisfactory fit to the ^{44}Ca$-^{40}$Ca difference data using either form of the potential. To reasonably fit the difference data, the diffuseness of the real and imaginary parts of the ^{44}Ca potential had to be increased. A similar increase was needed for the ^{142}Ce$-^{140}$Ce cross section difference analyzed previously (Ref. 3). In both cases neutrons are being added beyond closed neutron shells ($N=20$ and $N=82$), implying both ^{44}Ca and ^{142}Ce might not be as spherical as their respective closed-shell isotopes. Our calculated value for the difference in rms radii for ^{44}Ca and ^{40}Ca is in agreement with that calculated from low energy alpha particle scattering.

ACKNOWLEDGMENTS

We would like to thank R. W. Bauer for his constant support and encouragement. This work was performed under the auspices of the U.S. Department of Energy by the Lawrence Livermore National Laboratory under Contract No. W-7405-ENG-48.

APPENDIX

In order to examine the sensitivity of our optical model results to the form of the potential used, we have fit our total cross section and difference data with another potential (referred to as SV in the main text) of the form

$$U(r)=V_R f(r)+iW_V f(r)+iW_D g(r) + V_{so}\left[\frac{\hbar}{m_\pi c}\right]^2 \frac{1}{r}\left|\frac{df}{dr}\right|\sigma\cdot\mathbf{l}\,,$$
$$f(r)=(1+e^{[(r-R)/a]})^{-1}\,, \tag{A1}$$
$$g(r)=4e^{[(r-R)/a]}(1+e^{[(r-R)/a]})^{-2}\,.$$

A search for an acceptable fit to the ^{40}Ca σ_T data using this potential yielded the following strengths (in MeV) and geometrical parameters (in fm):

$$V_R=-52.0+0.34E\ ; \tag{A2a}$$
$$W_V=0.0,\ E\le 7.5\ \text{MeV}\,,$$
$$W_V=1.2-0.16E,\ E>7.5\ \text{MeV}\ ; \tag{A2b}$$
$$W_D=-3.325-0.67E,\ E\le 11.5\ \text{MeV}\,,$$
$$W_D=-11.03,\ E>11.5\ \text{MeV}\ ; \tag{A2c}$$
$$R_R=1.233A^{1/3},\ a_R=0.70\,,$$
$$R_V=1.233A^{1/3},\ a_V=0.70\,, \tag{A2d}$$
$$R_D=1.242A^{1/3},\ a_D=0.48\ ;$$
$$V_S=-8.3\,,$$
$$R_S=1.242A^{1/3},\ a_S=0.70\,. \tag{A2e}$$

The calculation of σ_T^{40} using this potential is shown in Fig. 2. For the fit to the $\Delta\sigma_T$ data shown in Fig. 4, it was necessary to increase the diffuseness of the real potential and volume absorptive potential from 0.70 fm to 0.74 fm and, in addition, the diffuseness of the surface absorptive potential was changed from 0.48 fm to 0.50 fm. An asymmetry term of the form $(30-0.4E)\,(N-Z)/A$ was added to Eq. (A2a) and W_V was held to the constant value of -2.8 MeV above $E=25$ MeV. These changes are similar to those made to the OU potential.

[1]See, for example, *Proceedings of the Karlsruhe International Discussion Meeting,* edited by H. Rebel, H. J. Grils, and G. Schatz (Institüt für Angewandte Kernphysik, Karlsruhe, 1979).

[2]F. Petrovich, in *The (p,n) Reaction and the Nucleon-Nucleus Force,* edited by C. D. Goodman, S. M. Austin, S. D. Bloom, J. Rapaport, and G. R. Satchler (Plenum, New York, 1979), p. 115.

[3]H. S. Camarda, T. W. Phillips, and R. M. White, Phys. Rev. C **29**, 2106 (1984).

[4]R. B. Schwartz, R. A. Schrack, and H. T. Heaton, *MeV Total Neutron Cross Sections,* Natl. Bur. Stand. (U.S.) Monograph 138 (U.S. GPO, Washington, D.C., 1974).

[5]S. Cierjacks *et al., High Resolution Total Neutron Cross-Sections Between 0.5-30 MeV* (Gesellschaft für Kernforschung, Karlsruhe, 1969).

[6]C. I. Zanelli *et al.,* Phys. Rev. C **23**, 1015 (1981).

[7]J. Rapaport, V. Kulkarni, and R. W. Finlay, Nucl. Phys. **A330**, 15 (1979).

[8]M. E. Smith and H. S. Camarda, Lawrence Livermore National Laboratory Internal Report UCID-18737, 1980.

[9]F. Michel, see Ref. 1, p. 201.

[10]S. M. Austin *et al.,* Phys. Rev. C **19**, 1186 (1979).

[11]J. Friedrich, see Ref. 1, p. 22.